

Search for isospin-symmetry breaking in the $A = 62$ isovector triplet

R. E. Mihai ¹, A. S. Mare ^{1,2}, N. Mărginean ¹, A. Petrovici ^{1,2}, O. Andrei,¹ M. Boromiza,¹ D. Bucurescu,¹ G. Căta-Danil,¹ C. Clisu,¹ C. Costache,¹ I. Dinescu,¹ D. Filipescu,¹ N. Florea,¹ I. Gheorghe,¹ A. Ionescu,¹ R. Lică,^{1,3} R. Mărginean,¹ C. Mihai,¹ A. Mitu,¹ A. Negret,¹ C. R. Niță,¹ A. Olăcel,¹ A. Oprea,¹ S. Pascu,^{1,3} A. Șerban,¹ C. Sotty,¹ L. Stan,¹ R. Șuvăilă,¹ S. Toma,¹ A. Turturică,¹ S. Ujeniuc,¹ and C. A. Ur⁴

¹Horia Hulubei National Institute of Physics and Nuclear Engineering - IFIN-HH, Bucharest, 077125, Romania

²Faculty of Physics, University of Bucharest, R-077125 Bucharest, Romania

³CERN, CH-1211 Geneva 23, Switzerland

⁴IFIN-HH/ELI-NP, 077125 Bucharest, Romania



(Received 13 September 2021; revised 4 April 2022; accepted 1 August 2022; published 26 August 2022)

The assignment of the first 2^+ state in ^{62}Ga has long been debated, due to its implications in triplet energy difference systematics in this mass region. An experiment has been performed at the IFIN-HH 9-MV Tandem accelerator using the ROSPHERE array in a mixed configuration of $\text{LaBr}_3(\text{Ce})$ and HPGe detectors, as well as an additional array of liquid scintillator neutron detectors. Excited states in ^{62}Ga were populated through a $2n$ fusion-evaporation channel and an anisotropy ratio was obtained from neutron-filtered HPGe statistics of transitions observed at different angles. A 2^+ state has been confirmed at an excitation energy of 978.1(1) keV. Theoretically, the interplay between isospin-symmetry breaking and shape-coexistence effects in the $A = 62$ isovector triplet is self-consistently treated within the beyond-mean-field complex excited Vampir variational model with symmetry projection before variation using an effective interaction obtained from a G matrix based on the charge-dependent Bonn CD potential adding the Coulomb interaction between the valence protons. Results are presented on Coulomb energy differences, mirror energy differences, triplet energy differences, and the superallowed Fermi β decay of the ground state of ^{62}Ge and ^{62}Ga .

DOI: [10.1103/PhysRevC.106.024332](https://doi.org/10.1103/PhysRevC.106.024332)

I. INTRODUCTION

It is generally true that energetically most favored states are those for which the isospin quantum number is equal to its projection on the third axis in the abstract isospin space. The most notable exceptions are odd-odd self-conjugate nuclei, where states of $T = 0$ and $T = 1$ coexist at low energies, the $T = 1, 0^+$ becoming even the ground state for those with $A > 58$.

While the light self-conjugate systems are easily understood within the quasideuteron scheme [1,2], it is much more complicated to theoretically describe systems containing several tens of nucleons. As the stability line drifts towards more neutron-rich nuclei, it also becomes increasingly difficult to produce heavy self-conjugate systems. Complex experimental measurements are needed to obtain partial information that could help the theoretical models to better predict nuclear behavior of such systems.

In nuclei, the isospin-symmetry breaking occurs due to the Coulomb interaction between protons and isospin violations in the strong interaction arising from the mass difference between the up and down quarks along with electromagnetic effects. The study of charge-symmetry and charge-independence breaking has been the subject of continuous effort investigating different isospin-related phenomena such as Coulomb energy differences (CED), mirror energy

differences (MED), triplet energy differences (TED) [3–6], as well as the isospin-symmetry violation effects on the superallowed Fermi β decay [7–9] among the nuclei of the isovector triplet. In the $A \approx 70$ mass region these tiny effects are created by the interplay between isospin-symmetry-breaking interactions and shape coexistence effects [4,6].

By dividing the TED to the mean value of the three energies of the excited states, one can obtain fractional TEDs. A systematic comparison between fractional TEDs for the first 2^+ states of $T = 1$ reveals apparent boundaries to these values, at least while taking into account nuclear masses in the $22 < A < 74$ mass range [10], with the exception of a significant dip for $A = 62$. Doubts of this data point placement within the systematics further arise if one takes into account the history of tentative 2^+ spin and parity assignment in ^{62}Ga . The paper by Rudolph *et al.* [11] published in 2004 discusses the existence of an 1017-keV excited state as the first 2^+ in ^{62}Ga , which decays through a 446-keV isovector $M1$ transition. No direct transition to the ground state was observed in this work and it has been interpreted that this decay pattern is strongly dependent on the size of the $2p_{3/2}$ component in the wave function, which favors strong $M1$ transitions.

This assignment was not contested nor discussed until David *et al.* published the results obtained in an experiment at GAMMASPHERE [12], where γ rays from ^{62}Ga were

detected through β -decay tagging following recoil mass identification. In this work, the 1017-keV level maintained its 2^+ assignment, but it was pointed out that a direct transition should have been observed, according to theoretical predictions, although it was not consistent with their spectra. Another notable finding was the observation of a 979-keV level decaying directly to the ground state. This newly observed level obtained a (1^+) assignment based on the 0.77(25) anisotropy ratio for detected γ rays at 32° and 90° with respect to the beam axis.

Later, Grodner *et al.* [13] published a third study on ^{62}Ga produced through the β^+ decay of ^{62}Ge . In this study, both 1017.1(4)-keV and 978.0(4)-keV states were observed, but were only given a tentative (1^+) assignment. The 1017.1(4)-keV level was observed decaying directly to the ground state, but due to the strong 511-keV electron-positron annihilation line in their spectrum, it was not possible to observe the decay pattern through the 447-keV transition. It was therefore inferred that at 1017.1(4) keV there could be a doublet of levels consistent with the one observed in Ref. [11]. More assessments can be made from this work by looking at transition probabilities. Thanks to their reported $B(GT)$ upper limit of 0.070(17) for the decay to the first ($T = 0$) 1^+ at 571 keV, one can deduce a value of 0.043 W.u. for the isovector $B(M1; 1^+ \rightarrow 0^+_{gs})$ through the $B(GT) - B(M1)$ proportionality relationship described by Fujita *et al.* [14]. This value is normally larger than that of the isovector $B(M1; 2^+ \rightarrow 1^+)$, which should not exceed 0.026 W.u. Moreover, if comparing with values for ^{62}Zn [15], the expected $B(E2; 2^+ \rightarrow 0^+)$ is of about 15 W.u. All of these arguments lead to the conclusion that the ($T = 1$) 2^+ state should not decay mainly through an isovector magnetic dipole.

Henry *et al.* [10] published another study on ^{62}Ga , which was produced in a ^{64}Ga two-neutron knockout reaction with secondary radioactive beams. Once again, a significant 977(2)-keV line was observed, questioning the previous assignments of the first ($T = 1$) 2^+ state in ^{62}Ga . This is when the systematics of fractional TED comes into play, questioning the fact that a 1017-keV state could be the first 2^+ in ^{62}Ga , as it places the data point far outside the region containing all values attributed to the $A = 22$ –74 mass range. The $2n$ -knockout mechanism significantly favors 2^+ state population as compared to other methods, but the 1017-keV transition was not even observed in the experiment. Therefore, the 977(2)-keV level was proposed as the new candidate for the first ($T = 1$) 2^+ state, although it was not possible to demonstrate that its transition to the ground state is in fact an electric quadrupole.

Finally, we mention the recent puzzling findings of Orrigo *et al.* [16]. In their paper, they maintain the 1^+ spin assignment for the 978-keV state observed from the β decay of ^{62}Ge while also giving a (1^+) assignment for the 1017-keV state, previously considered the first 2^+ in ^{62}Ga .

As a summary of all assessments that could be made from these studies, there are two candidate levels at 978 keV and at 1017 keV for the first ($T = 1$) 2^+ state in ^{62}Ga , prompting the need for clarification.

Theoretically, aiming to a comprehensive understanding of isospin-symmetry-breaking effects on the structure and

dynamics of exotic nuclei, we described successfully isospin-related phenomena in $A = 66, 70, 74,$ and 82 analogs [4,6,7] in the framework of the complex excited Vampir model. A difficult task for the theoretical models is the simultaneous description of the structure and superallowed Fermi β -decay distributions in the isovector triplet. The beyond-mean-field complex excited Vampir model allows for a unified description of structure and β -decay properties including in the projected mean fields neutron-proton correlations in both the $T = 1$ and $T = 0$ channels and general two-nucleon unnatural-parity correlations [17,18]. In the present study we will examine the isospin-symmetry-breaking effects on CED, MED, TED, and superallowed Fermi β decay for the $^{62}\text{Ge}, ^{62}\text{Ga}, ^{62}\text{Zn}$ triplet using the complex excited Vampir variational approach based on an effective interaction obtained from a G matrix starting from the charge-dependent Bonn CD potential adding the Coulomb interaction between the valence protons [6].

II. EXPERIMENT AND ANALYSIS

An experiment was performed at IFIN-HH, where excited states of ^{62}Ga were populated through the $^{58}\text{Ni}(^6\text{Li}, 2n)^{62}\text{Ga}$ fusion-evaporation reaction. CASCADE [19] calculations were performed, predicting a 5-mb cross section in the incident 19–22 MeV energy range, representing one percent of the total fusion cross section. The incident ^6Li beam energy of 22 MeV was chosen so that ^{62}Ga would be the only two-neutron evaporating channel. A beam intensity of 1.5 nA was chosen to minimize the dead time-induced count losses of the acquisition system while also avoiding HPGe signal pileup. Due to the reduced stopping power of ^6Li in nickel, a 5-mg/cm² ^{58}Ni target deposited on a 5-mg/cm² layer of ^{197}Au was used. The nickel layer corresponded to a 3-MeV beam energy loss, allowing the integration over the total effective cross section. The target was produced in the IFIN-HH target laboratory [20].

γ rays were detected with the ROSPHERE array [21] configured to allow coupling with three subarrays of neutron detectors in order to provide a clean tagging of events from neutron-evaporating exit channels. The subarrays consisted of two distinct liquid scintillator neutron detector walls containing 12 detectors each and placed at the two sides of ROSPHERE as close as possible to the reaction chamber and a third array of four neutron detectors at the 37° ring of ROSPHERE for maximum neutron detection efficiency. The total neutron detection efficiency of the liquid scintillator array was estimated at 4%. Ten Compton-suppressed HPGe detectors were placed as follows: One in the remaining spot at 37° , four at the supplementary 143° angle, and five at 90° . This placement allows us to obtain angular distribution ratios for the potential $E2$ candidates. The rest of the array was filled by 11 LaBr₃(Ce) detectors.

In the analysis process, we first used the liquid scintillator detector γ -neutron discrimination spectra to carefully select the neutron-evaporating exit channels. This acted as a highly efficient neutron filter, dampening the non-neutron-yielding exit channel γ lines by a factor of 300 when gating on one neutron. As seen in the top section of Fig. 1, the most promi-

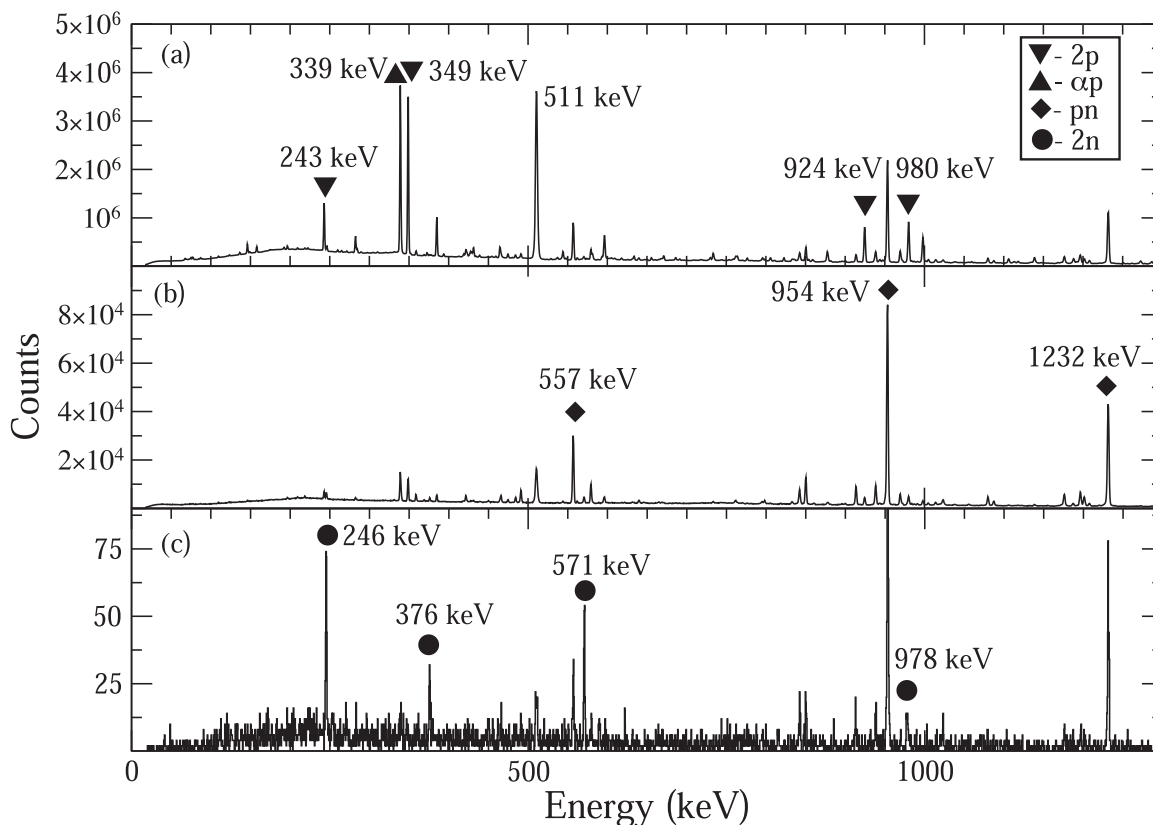


FIG. 1. (a) Total HPGe energy spectrum of the $^{58}\text{Ni} + ^6\text{Li}$ experiment. (b) One-neutron-gated HPGe energy spectrum. (c) Two-neutron-gated HPGe energy spectrum. The highlighted γ lines belong to nuclei from the main fusion-evaporation channels, namely, $^{62}\text{Cu}(2p)$, $^{59}\text{Ni}(\alpha p)$, $^{62}\text{Zn}(pn)$, as well as the weaker populated $^{62}\text{Ga}(2n)$.

ment γ lines come from proton-evaporating exit channels. By applying a one-neutron condition, the energy spectrum reveals the most intense γ lines of ^{62}Ga . A partial level scheme of ^{62}Ga showing the γ lines observed in the experiment is presented in Fig. 2, while their relative intensities are presented in Table I.

The neutron-gated HPGe statistics was then divided into two distinct unidimensional projections, one containing events from the four detectors at 90° and the other containing the statistics gathered by the six detectors placed at 143° and 37° angles. The projections were then compared and peaks were fitted to obtain the number of counts for both cases.

First, one cannot conclude whether the 1017-keV transition can be observed within the data due to the possible overlap with the Doppler-shifted 1023-keV transition from ^{62}Zn . Secondly, a 978.1-keV transition clearly emerges from background, as seen in Fig. 3. Taking in consideration the earlier mentioned cross-section calculations, the only sensible assumptions for the existence of a 978.1-keV line in the spectrum would be the deexcitation of either ^{63}Ga or ^{62}Ga , respectively. In the case of the former nucleus, much more intense transitions should also be seen within the spectrum. As seen in Fig. 4, contaminant lines from the 2n-gated γ spectrum were identified as coming from other well-studied nuclei, all of which are not known to yield 978-keV transitions. This only leaves room for the statement that we are indeed populating the 978.1-keV level in ^{62}Ga . No true co-

incidences with other transitions in ^{62}Ga are observed when gating on the 978.1-keV line, leading to the assumption that

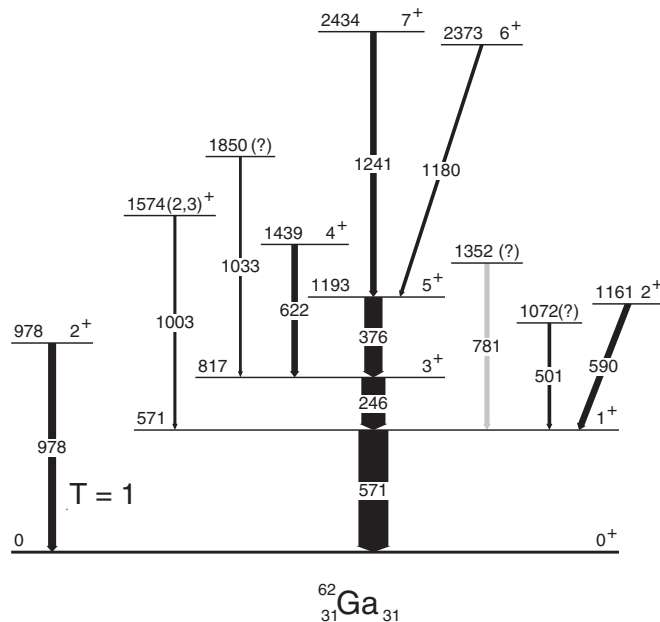


FIG. 2. ^{62}Ga partial level scheme containing all observed γ lines in current experiment. The 781-keV transition colored in light gray has been observed for the first time.

TABLE I. A listing of ^{62}Ga transitions and their relative intensities observed in this work. Values noted with an asterisk are estimated using γ -ray coincidences.

E_x (keV)	E_γ (keV)	I_{rel} (%)	I_i^π	I_f^π
571.2(1)	571.2(1)	100(3)	1^+	0^+
817.3(1)	246.0(1)	61(2)	3^+	1^+
978.1(1)	978.1(1)	27(2)	2^+	0^+
1072.5(1)	501.3(1)	5(2)*		1^+
1161.0(1)	589.8(1)	20(2)*	2^+	1^+
1193.8(2)	376.5(1)	37(2)	5^+	3^+
1352.0(1)	780.8(1)	6(3)*		1^+
1439.2(2)	621.9(2)	20(6)	4^+	3^+
1574.3(1)	1003.1(1)	4(1)*	$(2,3)^+$	1^+
1850.2(3)	1032.9(3)	3(1)*		3^+
2374.4(3)	1180.6(2)	10(4)*	6^+	5^+
2434.8(3)	1241.0(2)	33(7)*	7^+	5^+

this transition indeed deexcites the nucleus to the ground state.

To obtain an angular anisotropy ratio, it was necessary to also factor in the energy-specific detection efficiency per ring to the $I_{(37^\circ+143^\circ)} = 3189(264)$ counts and $I_{(90^\circ)} = 1081(157)$ counts. Calibration data with a ^{152}Eu source were taken after the experiment, allowing a precise determination of detection efficiency near the energy of interest due to the 964-keV ($1^- \rightarrow 2^+$) transition in ^{152}Sm . We report an experimental value of $R_{90^\circ/(37^\circ+143^\circ)} = 0.80(13)$.

Reference values of 0.84(3) and 1.26(4) were obtained for $R_{90^\circ/(37^\circ+143^\circ)}$ anisotropy ratios associated to pure quadrupole and dipole transitions, respectively, in ^{62}Zn , a nucleus coming from a much more productive fusion-evaporation channel. To further test the accuracy of the method, the multipolarities

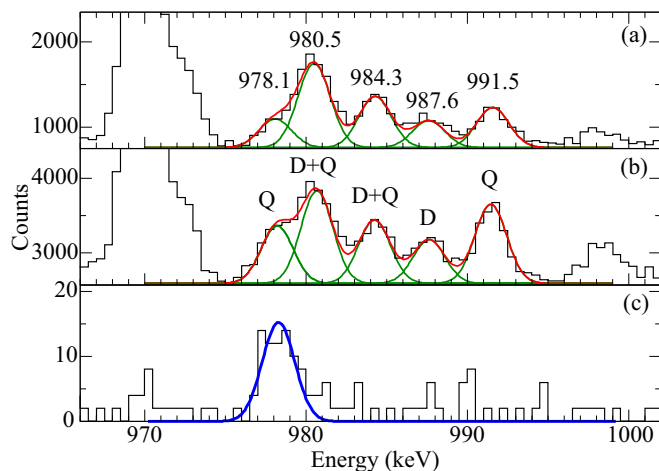


FIG. 3. (a) One-neutron-gated partial spectrum containing the statistics from detectors placed at 90° . (b) One-neutron-gated partial spectrum containing statistics from detectors placed at the 37° and supplementary 143° angles. (c) Two-neutron-gated partial spectrum containing statistics from all HPGe detectors. The multipolarities of the five transitions in the 978–992 keV energy range, presented in (b), were determined through $R_{90^\circ/(37^\circ+143^\circ)}$ angular anisotropy ratios.

ties of the four transitions in the 980–992-keV range were probed and found in agreement with the literature [22–25]. The obtained values are presented in Table II. The ratio corresponding to the 978-keV transition therefore reveals a level of anisotropy specific to an electric quadrupolar transition.

This represents substantial evidence to conclude that the observed 978.1-keV $E2$ transition directly links the ground state to a $J^\pi = 2^+$ state of the lowest yet reported excitation energy, confirming the assumptions made by Henry *et al.* [10]. We assume that the state observed in our experiment is different from the one of 978.3(1) keV reported in Ref. [16]. Moreover, this newly observed 2^+ state places $A = 62$ within the systematics of fractional triplet energy differences.

III. BEYOND-MEAN-FIELD VAMPIR CALCULATIONS

The complex excited Vampir (EXVAM) model uses Hartree-Fock-Bogoliubov (HFB) vacua as basic building blocks, which are only restricted by time-reversal and axial symmetry. The underlying HFB transformations are essentially complex and do mix proton with neutron states as well as states of different parity and angular momentum. The broken symmetries of these vacua (nucleon numbers, parity, total angular momentum) are restored by projection techniques and the resulting symmetry-projected configurations are used as trial wave functions in chains of successive variational calculations to determine the underlying HFB transformations as well as the configuration mixing. The HFB vacua of the above type account for arbitrary two-nucleon correlations and thus simultaneously describe like-nucleon as well as isovector and isoscalar neutron-proton pairing correlations.

For nuclei in the $A = 60$ –80 mass region we use a ^{40}Ca core and include the $1p_{1/2}$, $1p_{3/2}$, $0f_{5/2}$, $0f_{7/2}$, $1d_{5/2}$, and $0g_{9/2}$ oscillator orbits for both protons and neutrons in the valence space. We start with an isospin symmetric basis and then introduce the Coulomb shifts for the proton single-particle levels resulting from the ^{40}Ca core.

The effective two-body interaction is constructed from a nuclear matter G matrix based on the charge-dependent Bonn CD potential. In order to enhance the pairing correlations this G matrix was modified by adding short-range Gaussians in the $T = 0$ and $T = 1$ channels. In addition, the isoscalar interaction was modified by monopole shifts [6]. The Hamiltonian includes the two-body matrix elements of the Coulomb interaction between the valence protons.

In the isovector triplets the Coulomb energy differences are defined by $CED(J) = E_x(J, T = 1, T_z = 0) - E_x(J, T = 1, T_z = 1, T_z = 1)$, the mirror energy differences by $MED(J) = E_x(J, T = 1, T_z = -1) - E_x(J, T = 1, T_z = 1)$, and the triplet energy differences by $TED(J) = E_x(J, T = 1, T_z = -1) + E_x(J, T = 1, T_z = 1) - 2E_x(J, T = 1, T_z = 0)$, where E_x represents the excitation energy and $T_z = -1$ for the proton-proton pair. Assuming isospin symmetry the isobaric analog states will be degenerate. Breaking this symmetry leads to observable differences between energy levels of analog states. The CED, MED, TED are regarded as fingerprints of isospin-symmetry breaking in the effective interaction. In order to investigate the CED, MED, and TED in the $A = 62$ isovector triplet we calculated up to 20

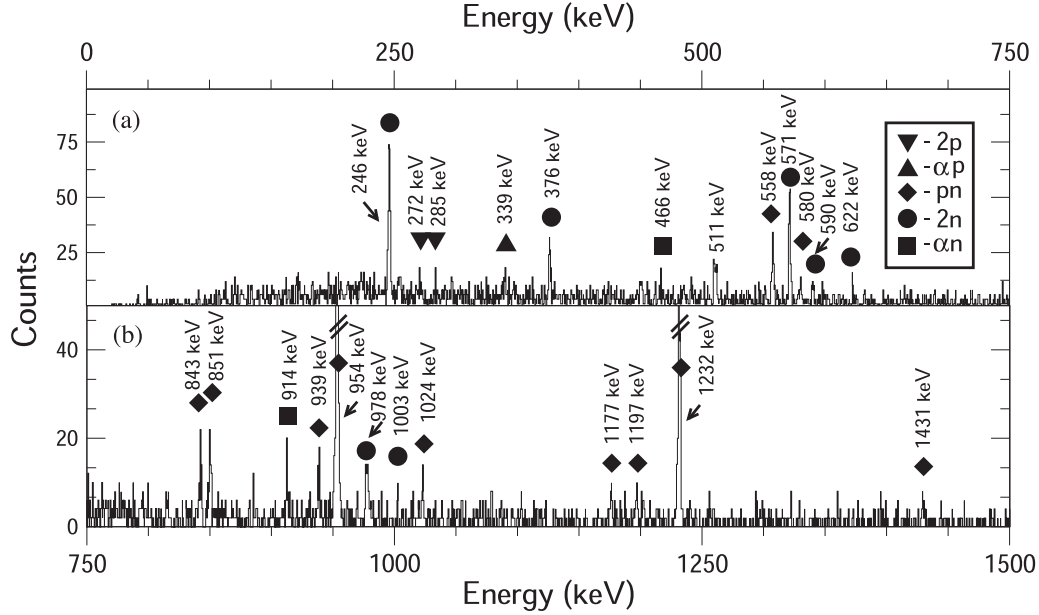


FIG. 4. 2n-gated HPGe energy spectrum in the (a) 0–750 keV and (b) 750–1500 keV energy ranges. The labeled γ lines have been identified as transitions belonging to the weakly populated $^{62}\text{Ga}(2n)$ and contaminants $^{62}\text{Cu}(2p)$, $^{59}\text{Ni}(\alpha p)$, $^{62}\text{Zn}(pn)$, and $^{59}\text{Cu}(\alpha n)$.

many-nucleon excited Vampir configurations for the spin 0^+ , 2^+ , and 4^+ in ^{62}Ge , ^{62}Ga , and ^{62}Zn using the above defined Hamiltonian. First, the Vampir solutions, representing the optimal mean-field description of the yrast states by single symmetry-projected HFB determinants, have been obtained. Subsequently, the excited Vampir approach was used to construct additional excited states by independent variational calculations. The final solutions for each spin have been obtained diagonalizing the residual interaction between the successively constructed orthogonal many-nucleon excited Vampir configurations. The variational procedure that we use involves projection before variation on particle number, angular momentum, and parity.

The results concerning the structure of the investigated 0^+ , 2^+ , and 4^+ states indicate a variable mixing of differently deformed prolate and oblate (β_2 varied from 0.09–0.19 and from -0.03 to -0.18) configurations in the intrinsic system in the final wave functions. The main configuration in the structure of the ground state represented $\approx 94\%$, while the amount of mixing for the yrast 2^+ and 4^+ states varied from 10%–14% in

TABLE II. Angular anisotropy ratio values ($R_{90^\circ/(37^\circ+143^\circ)}$) along with the multipolarities (M_γ) determined for transitions observed in this study.

Nucleus	E_γ (keV)	$I_i^\pi \rightarrow I_f^\pi$	$R_{90^\circ/(37^\circ+143^\circ)}$	M_γ
^{62}Zn	953.75(2)	$2^+ \rightarrow 0^+$	0.84(3)	Q
^{62}Zn	1857.5(4)	$(5)^- \rightarrow 4^+$	1.26(4)	D
^{62}Ga	978.1(1)	$2^+ \rightarrow 0^+$	0.80(13)	Q
^{62}Cu	980.5(2)	$5^+ \rightarrow 4^+$	1.91(14)	D+Q
^{61}Cu	984.3(2)	$9/2^- \rightarrow 7/2^-$	1.73(16)	D+Q
^{61}Cu	987.6(1)	$9/2^+ \rightarrow 7/2^-$	1.37(17)	D
^{64}Zn	991.5(1)	$2^+ \rightarrow 0^+$	0.99(9)	Q

the isovector triplet ^{62}Ge , ^{62}Ga , ^{62}Zn . In Table III is indicated the contribution of the EXVAM configurations bringing at least 1% to the total amplitude of the corresponding wave functions in ^{62}Ga .

In Fig. 5 we present the complex excited Vampir spectra for the $A = 62$ triplet compared with the available data. For a comparison to the measured electromagnetic properties of the yrast states in ^{62}Zn we calculated $B(E2)$ transition strengths and g factors. The $B(E2; I \rightarrow I - 2)$ values evaluated using as effective charges $e_p = 1.5$ and $e_n = 0.5$ are presented in Table IV. The measured g factor of the yrast 2^+ state is 0.37 (10) [26], while the EXVAM value amounts to 0.56. Results obtained by large-scale shell model calculations for $B(E2)$ values and g factors indicate agreement with present data [27,28].

Figure 6 illustrates the complex excited Vampir Coulomb energy differences for the ^{62}Ga – ^{62}Zn analogs obtained using the above defined Hamiltonian compared to the data including the present experimental result.

Figure 7 presents the complex excited Vampir predictions on mirror energy differences and triplet energy differences for the $A = 62$ isovector triplet compared to the available experimental results. The EXVAM trend manifested in CED, MED, and TED indicates agreement with the experimental available data giving support to the involved effective inter-

TABLE III. The amount of mixing for the lowest complex excited Vampir states in ^{62}Ga .

$I(\hbar)$	Prolate content	Oblate content
0^+	94(2)(1)(1)%	1%
2^+	91(4)(2)%	2(1)%
4^+	90(4)(2)(1)(1)%	1%

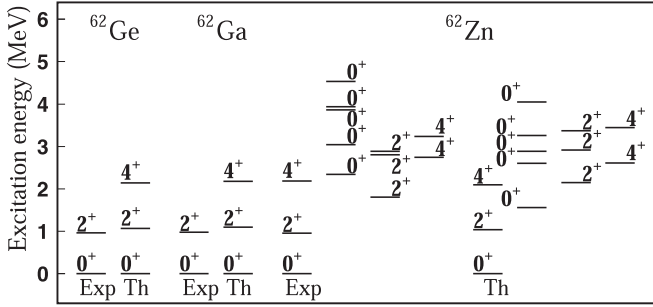


FIG. 5. The complex excited Vampir spectra for the analog states in ^{62}Ge , ^{62}Ga , and ^{62}Zn and the lowest few 0^+ , 2^+ , and 4^+ states in ^{62}Zn compared with the available data.

action and the beyond-mean-field complex excited Vampir model. It is worthwhile to mention that it is difficult to disentangle between the effects of the isospin-symmetry-breaking interactions and the shape coexistence and mixing.

For a comprehensive understanding of the isospin-symmetry-breaking related phenomena we used the same approach and effective interaction to obtain by independent chains of variational calculations the wave functions of the 0^+ states involved in the superallowed Fermi β decay of the ground state of ^{62}Ge and ^{62}Ga .

The Fermi reduced transition probability is written as

$$B_{if}(F) = \frac{1}{2J_i + 1} |M_F|^2, \quad (1)$$

where the nuclear matrix elements between the initial ($|\xi_i J_i\rangle$) and the final ($|\xi_f J_f\rangle$) states of spin J_i and J_f , respectively

$$\begin{aligned} M_F &\equiv \langle \xi_f J_f | \hat{1} | \xi_i J_i \rangle \\ &= \delta_{J_i J_f} \sum_{ab} M_F(ab) \langle \xi_f J_f | [c_a^\dagger \tilde{c}_b]_0 | \xi_i J_i \rangle, \end{aligned} \quad (2)$$

are composed of the reduced single-particle matrix elements of the unit operator $\hat{1}$, $M_F(ab) = \langle a | \hat{1} | b \rangle$, and the reduced one-body transition densities calculated using the harmonic oscillator wave functions. For the β^+ decay c_a^\dagger is the neutron creation operator and \tilde{c}_b is the proton annihilation operator and the sum runs over the valence nucleons. It is worthwhile to mention that the involved 0^+ states are calculated independently for each nucleus. In the isospin-symmetry limit the Fermi matrix element squared for the $T = 1$ emitters is $|M_{F_{is}}|^2 = 2$. The isospin-symmetry-breaking correction is defined as a deviation of the realistic Fermi matrix element from this value $|M_F|^2 = |M_{F_{is}}|^2 (1 - \delta_c)$. If the isospin-symmetry is broken nonanalog Fermi β -decay branches emerge. Our

TABLE IV. $B(E2; I \rightarrow I - 2)$ values (in $e^2\text{fm}^4$) for the yrast states in ^{62}Ge , ^{62}Ga , and ^{62}Zn .

$I[\hbar]$	^{62}Ge		^{62}Zn	
	EXVAM	EXVAM	EXVAM	Expt.
2^+	266	250	238	245 (12)
4^+	345	321	302	379 (+102/-175)

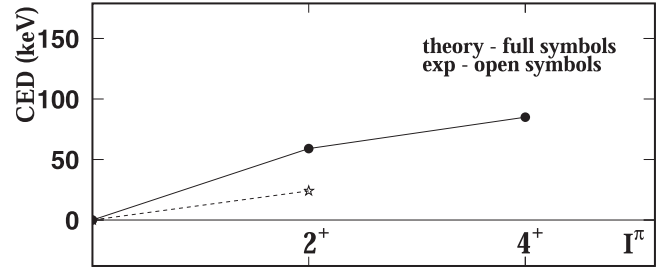


FIG. 6. Comparison of the complex excited Vampir results for CED to the experimental data.

EXVAM theoretical results indicate that the depletion of the ground-to-ground transition amounts to 0.74% for the ^{62}Ge and 0.75% for the ^{62}Ga ground-state decay and the missing strength is distributed over many 0^+ excited states. In Fig. 8 is displayed the Fermi strength distribution for the decay of the ground state of ^{62}Ga to 0^+ states in ^{62}Zn . In agreement with recent experiments [9,29] EXVAM results reveal weak branches to the lowest few excited 0^+ states. The missing strength in the ground-to-ground superallowed Fermi β decay gives an upper limit for the isospin-symmetry violation, but one can not disentangle between the effects of isospin-symmetry-breaking interactions and shape coexistence and mixing.

The present investigation represents the first beyond-mean-field treatment of the $A = 62$ isovector triplet based on an effective two-body interaction constructed from a nuclear matter G matrix starting from the charge-dependent Bonn CD potential able to describe self-consistently the interplay between isospin-symmetry-breaking and shape coexistence and mixing effects.

IV. CONCLUSIONS

An experiment was performed at IFIN-HH where excited states in ^{62}Ga were populated through the $^{58}\text{Ni}(^6\text{Li}, 2n)$ fusion-evaporation reaction. The precise angular anisotropy ratio determined in this experiment for the 978.1-keV transition to the ground state in ^{62}Ga reveals that we have indeed populated the lowest-lying 2^+ state. This state's newly assigned spin and parity positions the $A = 62$ isovector triplet within the typical range of values in the $(T = 1)J^\pi = 2^+$ fractional TED systematics. In this work, we obtained the

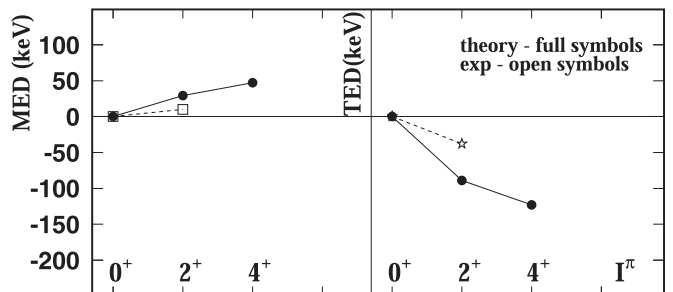


FIG. 7. The complex excited Vampir results for MED and TED in the $A = 62$ isovector triplet compared to data.

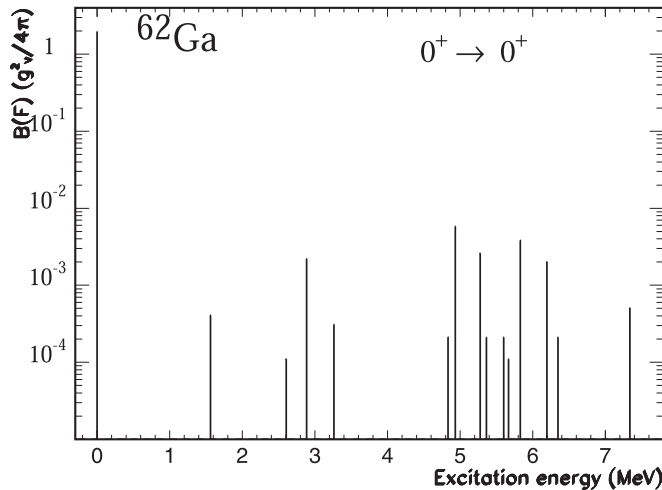


FIG. 8. The Fermi strength distribution for the decay of the ground state of ^{62}Ga to ^{62}Zn within the complex excited Vampir model.

first results on the effect of isospin mixing on CED, MED, TED, and superallowed Fermi β decay in the $A = 62$ isovector triplet calculating the 0^+ , 2^+ , and 4^+ states in these nuclei and the Fermi decay of the ground states of ^{62}Ge and ^{62}Ga

in the frame of the complex excited Vampir model, using an effective interaction obtained for the $A \approx 70$ mass region starting from the charge-dependent Bonn CD potential. For the first time we estimated the isospin-symmetry-breaking effects taking into account both the Coulomb interaction and the isospin-symmetry violation in the strong force as it is considered by the Bonn CD potential. The upper limit of 0.75% for the depletion of the ground-to-ground superallowed Fermi β decay includes both, the isospin-symmetry-breaking interactions and shape coexistence and mixing effects. The theoretical results indicate agreement with the experimental data on the discussed observables.

ACKNOWLEDGMENTS

This work was supported by the Ministry of Research, Innovation and Digitalization under Contracts No. 04FAIR/2020, No. PN-19-06-01-02, No. PN-IIIPI-1.1-TE-2019-0337. The authors of this paper would also like to thank the operators of the IFIN-HH 9-MV TANDEM accelerator for their dedication and professionalism in providing a high-quality ^6Li beam during the measurement time of this experiment.

The authors R.E.M. and A.S.M. contributed equally to this work.

-
- [1] T. Tagami, *Prog. Theor. Phys.* **21**, 533 (1959).
 [2] A. F. Lisetskiy, R. V. Jolos, N. Pietralla, and P. von Brentano, *Phys. Rev. C* **60**, 064310 (1999).
 [3] M. A. Bentley and S. M. Lenzi, *Prog. Part. Nucl. Phys.* **59**, 497 (2007).
 [4] G. de Angelis *et al.*, *Phys. Rev. C* **85**, 034320 (2012).
 [5] K. Kaneko, Y. Sun, T. Mizusaki, and S. Tazaki, *Phys. Rev. C* **89**, 031302(R) (2014).
 [6] A. Petrovici, *Phys. Rev. C* **91**, 014302 (2015).
 [7] A. Petrovici, K. W. Schmid, O. Radu, and A. Faessler, *Phys. Rev. C* **78**, 064311 (2008).
 [8] W. Satuła, J. Dobaczewski, W. Nazarewicz, and T. R. Werner, *Phys. Rev. C* **86**, 054316 (2012).
 [9] J. C. Hardy and I. S. Towner, *Phys. Rev. C* **102**, 045501 (2020).
 [10] T. W. Henry *et al.*, *Phys. Rev. C* **92**, 024315 (2015).
 [11] D. Rudolph *et al.*, *Phys. Rev. C* **69**, 034309 (2004).
 [12] H. M. David *et al.*, *Phys. Lett. B* **726**, 665 (2013).
 [13] E. Grodner *et al.*, *Phys. Rev. Lett.* **113**, 092501 (2014).
 [14] Y. Fujita *et al.*, *Prog. Part. Nucl. Phys.* **66**, 549 (2011).
 [15] B. Pritychenko *et al.*, *Nucl. Instrum. Meth. Phys. Res. A* **640**, 213 (2011).
 [16] S. E. A. Orrigo *et al.*, *Phys. Rev. C* **103**, 014324 (2021).
 [17] A. Petrovici and O. Andrei, *Phys. Rev. C* **92**, 064305 (2015).
 [18] A. Petrovici, *Phys. Rev. C* **97**, 024313 (2018).
 [19] V. S. Barashenkov *et al.*, *At. Energ.* **87**, 742 (1999).
 [20] N. Florea *et al.*, *J. Radioanal. Nucl. Chem.* **305**, 707 (2015).
 [21] D. Bucurescu *et al.*, *Nucl. Instrum. Meth. Phys. Res. A* **837**, 1 (2016).
 [22] J. A. Tostevin and J. S. Al-Khalili, *Phys. Rev. C* **59**, R5 (1999).
 [23] D. G. Sarantites *et al.*, *Phys. Rev. C* **8**, 629 (1973).
 [24] D. N. Simister *et al.*, *J. Phys. G: Nucl. Phys.* **4**, 111 (1978).
 [25] D. N. Simister *et al.*, *J. Phys. G: Nucl. Phys.* **6**, 81 (1980).
 [26] A. L. Nichols, B. Singh, and J. K. Tuli, *Nucl. Data Sheets* **113**, 973 (2012).
 [27] O. Kenn, K. H. Speidel, R. Ernst, S. Schielke, S. Wagner, J. Gerber, P. Maier-Komor, and F. Nowacki, *Phys. Rev. C* **65**, 034308 (2002).
 [28] K. Moschner *et al.*, *Phys. Rev. C* **82**, 014301 (2010).
 [29] A. D. MacLean *et al.*, *Phys. Rev. C* **102**, 054325 (2020).